Current Science
CS 5 (6), 5454-5471 (2025)
Received 01 Nov 2025 | **Accepted 17 November** 2025 | **Online Available 26 November** 2025
https://doi.org/10.52845/CS/2025-5-6-14

Current Science

Current Science

OPEN ACCESS

ISSN (O) 2795-8639

Original Article

The Causal Relationship between Mirna and Colorectal Cancer: Result from Mendelian Randomization Study and RT-Qpcr Experiment Validation

Zhengqi Peng[1*], Arzoo Prasai[2*], Pengkhun Nov[2#], Mengchuan Wang[1#]

[1]Department of General Surgery, Zhujiang Hospital, Southern Medical University, Guangzhou, Guangdong, 510282, P.R. China.

[2]Department of Radiation Oncology, Oncology Center, Zhujiang Hospital, Southern Medical University, Guangzhou, Guangdong, 510282, P.R. China.

***These Authors Contributed Equally to this Work**

[#]Corresponding Author

***Corresponding Author: Pengkhun Nov, Mengchuan Wang**

Abstract:

Background: Colorectal cancer (CRC) is a major global health concern, and understanding its molecular underpinnings is essential for effective intervention strategies. This study investigates the causal relationship between microRNAs (miRNAs) and CRC using a Mendelian Randomization (MR) approach, complemented by reverse transcription quantitative polymerase chain reaction (RT-qPCR) validation.

Methods: We conducted an extensive two-sample MR analysis. Briefly, the publicly available genetic data were utilized for investigation of the causal association between 2803 miRNAs and CRC; the inverse variance weighted (IVW) model and weighted medians were employed for MR analyses; and sensitivity analyses were adopted for heterogeneity and pleiotropy assessments and further confirm with RT-qPCR experiment.

Results: Our analysis revealed a total of 86 miRNAs associated with CRC. Of them, miR−4274 [odds ratio (OR) = 1.554, 95% confidence interval (CI) = 1.181– 2.044, p = 0.002], miR−4769−3p (OR = 1.357, 95% CI=1.120–1.644, p = 0.002), and miR−6789−5p (OR = 1.508, 95% CI=1.040– 2.187, p = 0.030) were strongly associated with CRC risks. The RT-qPCR results further confirmed that the expression levels of miR-4274, miR-4769-3p, and miR-6789-5p were significantly higher in CRC cell lines (HCT116, HT29, and Caco-2) compared with normal colon epithelial cells (HIEC).

Conclusion: These insights pave the way for further research into the clinical applications of miRNAs in CRC, offering promising avenues for diagnosis and treatment.

Keywords: MicroRNA, Colorectal cancer, Mendelian randomization, GWAS.

1. Introduction

CRC is one of the leading causes of cancer-related morbidity and mortality worldwide [1]. Understanding the molecular mechanisms underlying CRC is crucial for developing effective prevention and treatment strategies [2]. miRNAs, small non-coding RNA molecules that regulate gene expression, have emerged as significant players in cancer biology [3]. They modulate various cellular processes, including proliferation, apoptosis, and metastasis, making them potential biomarkers and therapeutic targets in CRC [4, 5].

Emerging evidence suggests that alterations in miRNA expression profiles are associated with CRC progression and patient outcomes [6, 7].

However, establishing a causal relationship between specific miRNAs and CRC risk remains a challenge due to confounding factors in observational studies [8]. MR offers a robust approach to infer causality by using genetic variants as IVs [9]. This method helps mitigate biases from confounding and reverse causation, providing a clearer understanding of the relationship between miRNAs and CRC.

In this study, we aimed to elucidate the causal relationship between miRNAs and CRC using a MR framework. Additionally, we validated our findings through RT-qPCR experiments, providing further evidence of the role of miRNAs in CRC. By integrating genetic data with experimental validation, our research seeks to enhance the understanding of miRNA involvement in CRC and contribute to the identification of novel diagnostic and therapeutic avenues.

Research Gap / Hypothesis

Gap:

Despite numerous observational studies linking specific miRNAs to CRC prognosis and biology, causal inference remains limited. Conventional epidemiologic associations are susceptible to confounding, reverse causation, and measurement bias. While MR analyses can strengthen causal claims by using genetic instruments, MR findings for miRNAs in CRC are still sparse and often rely on limited instrument strength or available GWAS data. Additionally, experimental validation in cell lines (e.g., RT-qPCR in cell line) is frequently not integrated with robust causal inference, leaving a gap between statistical causality and mechanistic validation.

Hypothesis:

Causal Hypothesis (MR): Genetic proxies (cis- or trans-eQTLs) for specific miRNAs causally influence colorectal cancer risk and/or progression, such that higher genetically-predicted expression of oncogenic miRNAs increases CRC risk or aggressiveness, while higher expression of tumor-suppressive miRNAs decreases risk or progression.

Validation Hypothesis (RT-qPCR): In independent CRC patient samples and matched controls, differential expression levels of these miRNAs observed in MR analyses correspond to the direction and magnitude of effect, supporting a mechanistic link between miRNA dysregulation and CRC pathology.

Core Research Question:

Do genetically predicted expression levels of candidate miRNAs causally affect colorectal cancer risk and progression, and can RT-qPCR validation in cell lines samples corroborate these causal relationships?

Implications:

Establishing a causal role for specific miRNAs in CRC could identify robust biomarkers and therapeutic targets.

Demonstrating concordance between MR estimates and RT-qPCR data would strengthen evidence for translational relevance and mechanistic pathways.

Now we also updated the specific aim: This study aimed to identify microRNAs with a potential causal role in CRC using Mendelian randomization, followed by RT-qPCR validation in CRC cell lines.

2 Materials and Methods

2.1 Study Design

The causal relationship between 2,803 microRNA expression quantitative trait loci (miR-eQTLs) and CRC was evaluated using two-sample MR analyses. This approach utilized genetic variations as proxies for risk factors. For robust causal inference, the IVs used in MR must satisfy three essential criteria: (1) there should be a direct link between the genetic variant and the exposure; (2) the genetic variant must not be associated with any potential confounders that could affect the relationship between the exposure and the

outcome; and (3) the effect of the genetic variant on the outcome should operate solely through the exposure, without involvement of alternative pathways colorectal cancer downloaded from the GWAS dataset included 387,318 European individuals (4,562 cases and 382,756 controls) **(Figure 1)**. All Mendelian randomization analyses were conducted in accordance with the STROBE-MR guidelines (**Supplementary File 1**).

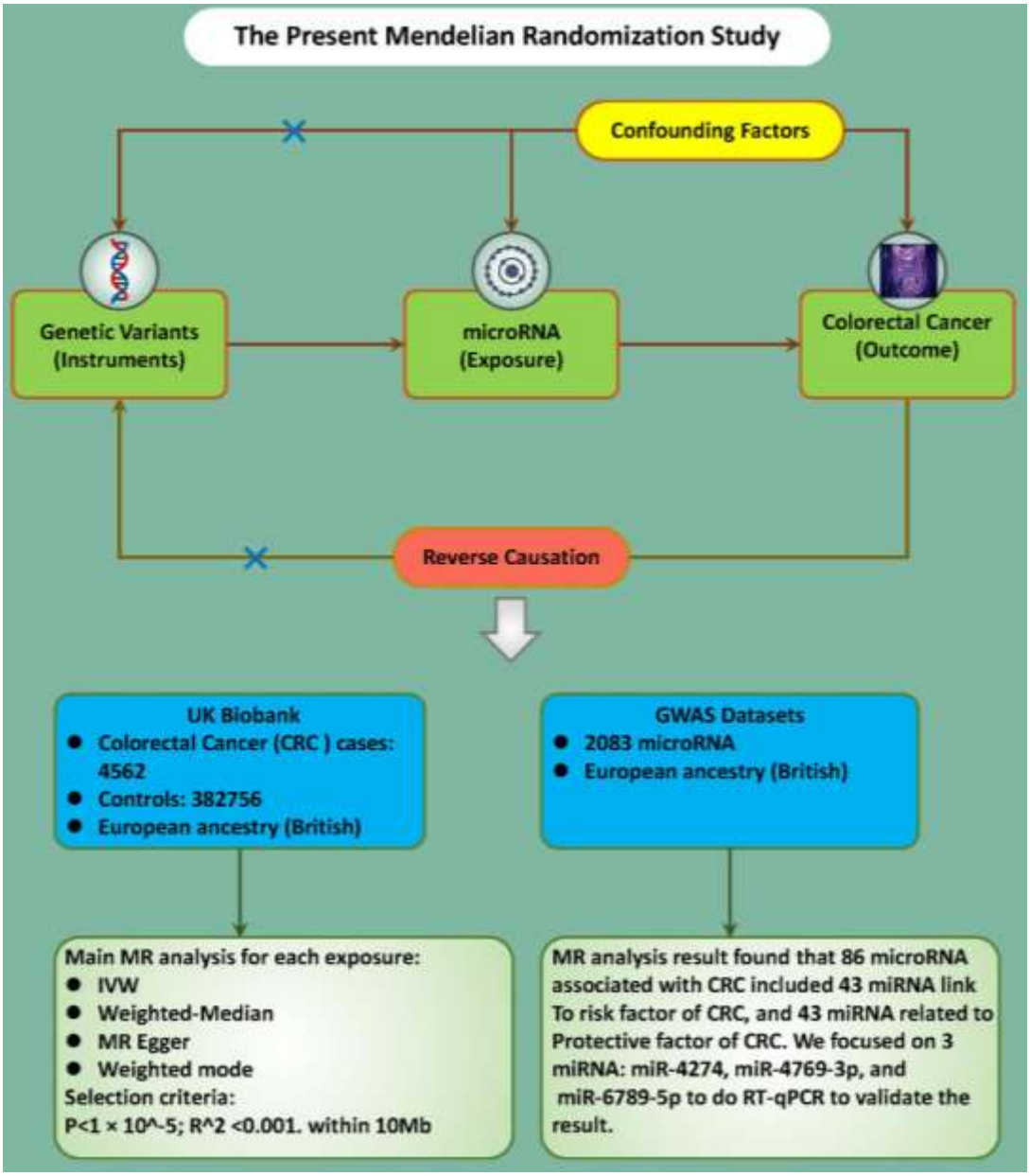

Figure 1. Study Design Flowchart.

2.2 Data sources for Exposure and Outcome

The exposure data originated from the research conducted by Huan et al. (2015) [10] and can download from the statistics summary of Genome-Wide Association Study (GWAS) (https://gwas.mrcieu.ac.uk/). In summary, this study aimed to uncover genetic variants linked to microRNA expression levels (known as microRNA expression quantitative trait loci or miR-eQTLs) using a sample of 5,239 participants from the Framingham Heart Study (FHS). The analysis accounted for age, sex, and cohort differences. Huan et al. identified a total of 9,612 variants associated with 76 mature miRNAs, with a false discovery rate (FDR) of less than 0.1. These genetic variants related to miRNAs expression served as instruments to investigate the causal connections between miRNAs and colorectal cancer. Referring to the ID of CRC,

related data were downloaded from UK Biobank pheweb database (https://pheweb.org/UKB-SAIGE/) including 387318 European individuals (n = 4562 case patients and 382756 control participants) for CRC.

2.3 Instrument Selection

Given the substantial number of single-nucleotide polymorphisms (SNPs) demonstrating genome-wide significance ($p < 5 \times 10^{-8}$) for miRNAs traits, we implemented stricter correlation thresholds ($p < 5 \times 10^{-9}$) for selecting genetic IVs. These IVs were classified using the Linkage Disequilibrium (LD) reference panel from the 1000 Genomes Project, applying a threshold of $R^2 < 0.001$. within a 10 MB range. Due to the relatively limited size of the GWAS data for miRNAs, we also considered a p-value cutoff of 1×10^{-5} and a more relaxed clustering threshold ($R^2 < 0.001$. at a distance of 10 MB) [11]. To ensure the robustness of our analysis, we focused on IVs with F-statistics exceeding 10, identifying them as strong instruments for further investigation. These IVs were extracted from summary statistics related to CRC outcomes, omitting any that showed potential pleiotropic effects ($p < 1 \times 10^{-5}$) on gastric cancer, adhering to methodologies from earlier studies [12]. To maintain consistency in our analysis, we aligned SNPs between the exposure and outcome datasets to ensure uniform effect estimates for the same effect allele [11].

2.4 Experiment Validation

2.4.1 Reagents and Instruments

Phosphate-buffered saline (PBS; Cat# G4202) was obtained from Servicebio (Wuhan, China). RPMI-1640 medium (Cat# PM150110) and fetal bovine serum (FBS; Cat# 164210-50) were purchased from Procell Life Science & Technology Co., Ltd. (Wuhan, China). Penicillin–streptomycin solution (Cat# C100C5) and 0.25% trypsin-EDTA (Cat# C100C1) were obtained from NCM Biotech (Suzhou, China). The miRNA First Strand cDNA Synthesis Kit (Tail Reaction, Cat# B532451) was purchased from Sangon Biotech (Shanghai) Co., Ltd. Real-time quantitative PCR was performed using 2 × EZ Color SYBR Green qPCR Master Mix (ROX2; Cat# A0012-R2; EZBioscience, United States).

2.4.2 Cell Culture

Human HIEC normal intestinal epithelial cells, along with HCT116, HT29, and CACO2 colorectal carcinoma cells, were purchased from Procell Life Science & Technology Co., Ltd. (Wuhan, China). Cells were cultured in RPMI-1640 medium supplemented with 10% fetal bovine serum, 10 U/mL penicillin, and 10 µg/mL streptomycin, and maintained at 37 °C in a humidified incubator with 5% CO_2. All cell lines were authenticated by short tandem repeat (STR) profiling and verified to be free of mycoplasma and cross-species contamination.

2.4.3 RNA Extraction

Total RNA was extracted from log-phase HIEC, HCT116, HT29, and CACO2 cells using standard phenol/chloroform procedures. Cells were washed twice with PBS and lysed with an appropriate volume of lysis buffer to ensure complete disruption. Following phase separation, the aqueous phase containing RNA was collected, and RNA was precipitated with isopropanol. The RNA pellet was centrifuged at 4 °C, washed with 75% ethanol, and dissolved in RNase-free water. RNA concentration and purity were assessed by spectrophotometry (A260/A280), and integrity was verified prior to downstream applications.

2.4.4 miRNA cDNA Synthesis

For cDNA synthesis, 2 µg of total RNA was reverse transcribed using the miRNA First Strand cDNA Synthesis Kit (Tail Reaction). The 20 µL reaction mixture contained 10 µL of 2× miRNA P-RT Solution Mix, 2 µL of miRNA P-RT Enzyme Mix, RNA template, and RNase-free water. The mixture was gently mixed, briefly centrifuged (3–5 s), and incubated at 37 °C for 60 minutes. Enzyme inactivation was performed at 85 °C for 5 minutes, and the resulting cDNA was stored at 4 °C. Prior to RT-qPCR, cDNA was diluted 50-fold and used as the template.

2.4.5 miRNA Primer Design

Mature miRNA sequences were retrieved from miRBase (https://www.mirbase.org/), and primers were designed using Vazyme miRNA primer design software (http://www.vazyme.com/companyfile/7/). Since reverse primers are universal, only forward primers were designed for each miRNA. All primers were verified for specificity prior to synthesis. Forward primer sequences included

Universal U6 Primer F (CTCGCTTCGGCAGCACA), miR-4274 Primer F (ATTACAGCAGTCCCTCCCCCT), miR-4769-3p Primer F (TTATTCTGCCATCCTCCCTCCCCTA), and miR-6789-5p Primer F (ATTATAAGTAGGGGCGTCCCGGGCG). The universal PCR reverse primer sequence was AACGCTTCACGAATTTGCGT.

2.4.6 Quantitative Reverse Transcription PCR (RT-qPCR)

RT-qPCR was performed using 2 × EZ Color SYBR Green qPCR Master Mix (ROX2) with miRNA-specific primers. Each 20 μL reaction contained 1 μL of cDNA template, 10 μL of 2 × SYBR Green Master Mix, and 0.3 μM of each forward and reverse primer. Cycling conditions were: initial denaturation at 95 °C for 10 minutes, followed by 40 cycles of 95 °C for 15 seconds and 60 °C for 1 minute. U6 miRNA was used as an internal reference gene, and all reactions were performed in triplicate.

2.5 Statistical Analysis

In the present study, multiple individual genetic variants were employed as IVs, rather than relying solely on a composite allele score. This strategy allowed for a more comprehensive evaluation of core MR assumptions, detection of potential pleiotropy, and improved performance in both sensitivity and multivariable MR analyses [13]. To evaluate the robustness of the causal estimates under varying assumptions regarding heterogeneity and pleiotropy, four complementary MR methods were applied: inverse variance weighted (IVW; random-effects model), weighted median, MR-Egger regression, and MR-PRESSO (pleiotropy residual sum and outlier). Among these, IVW served as the primary analytical framework across all four IV sets. Heterogeneity in the effect estimates was quantified using Cochran's Q statistic.

Additional analyses were conducted under more conservative assumptions. While the IVW method assumes the validity of all included variants, its estimates may be biased in the presence of extensive horizontal pleiotropy [14]. In contrast, the weighted median method remains consistent if at least 50% of the genetic instruments are valid, providing increased robustness against invalid instruments [15]. When over half of the variants demonstrated horizontal pleiotropy, the strength of the instruments was evaluated using F-statistics, where a mean F-statistic below 10 indicated the presence of weak instruments [16].

MR-Egger regression was utilized to assess directional pleiotropy; a non-zero intercept in this model would suggest violation of the IV assumption due to directional effects [17]. In addition, MR-PRESSO was employed to identify and correct for outlier SNPs that contributed disproportionately to heterogeneity (NbDistribution = 1,500) [18]. To further address reverse causation, Steiger filtering was performed to exclude variants with stronger associations with the outcome than with the exposure [19].

Expression levels of target miRNAs were quantified using the ΔΔCt method, with fold changes calculated as 2^(-ΔΔCt). All experiments were performed with a minimum of three independent replicates per group. Data are presented as mean ± standard error of the mean (SEM), and group differences were assessed using independent-sample t-tests. A two-sided P-value < 0.05 was considered statistically significant. Statistical significance is indicated as follows: ns, not significant; *P < 0.05, **P < 0.01, ***P < 0.001, ****P < 0.0001 vs. control.

The statistical power of the MR analyses was calculated using mRnd (https://cnsgenomics.shinyapps.io/mRnd/) (**Table S1**). All statistical analyses were performed using R version 4.3.2 (R Foundation) and specific R packages ("TwoSampleMR" and "MR") tailored for MR analysis. The TwoSampleMR package provided causal estimates from the four MR models (IVW, weighted median, MR-Egger, and MR-PRESSO), and the MR package was utilized for multivariable MR [20, 21]. RT-qPCR data processing and graphical visualization were

conducted with GraphPad Prism version 8 (GraphPad; Dotmatics).

3 Results

3.1 Causal Association between miRNAs and CRC

To investigate the causal effect of various metabolites on CRC, we conducted a two-sample MR analysis and utilized IVW as the primary analysis method. Our results showed the association between 86 miRNAs and CRC include 43 associated risk factors with CRC (**Figure 2**) and 43 related to protective factors (**Figure 3**), highlighting some of the strongest associations. Briefly, the CRC risk was strongly associated with miR−4274 [odds ratio (OR) = 1.554, 95% confidence interval (CI) = 1.181–2.044, p = 0.002], miR−4769−3p (OR = 1.357, 95% CI=1.120–1.644, p = 0.002), and miR−6789−5p (OR = 1.508, 95% CI=1.040–2.187, p = 0.030) (**Figure 4**).

Exposure	Method	No.of SNP	OR(95% CI)	P
miR−130a−3p	Inverse variance weighted	10	1.293 (1.123 to 1.490)	0.000
miR−5196−3p	Inverse variance weighted	9	1.266 (1.099 to 1.457)	0.001
miR−4274	Inverse variance weighted	6	1.554 (1.181 to 2.044)	0.002
miR−4769−3p	Inverse variance weighted	7	1.357 (1.120 to 1.644)	0.002
miR−3652	Inverse variance weighted	9	1.230 (1.073 to 1.410)	0.003
miR−1185−5p	Inverse variance weighted	14	1.164 (1.052 to 1.288)	0.003
miR−7158−3p	Inverse variance weighted	11	1.165 (1.047 to 1.295)	0.005
miR−4764−5p	Inverse variance weighted	9	1.167 (1.047 to 1.301)	0.005
miR−3679−5p	Inverse variance weighted	11	1.186 (1.051 to 1.337)	0.005
miR−3662	Inverse variance weighted	9	1.187 (1.049 to 1.342)	0.007
miR−6792−5p	Inverse variance weighted	5	1.220 (1.045 to 1.424)	0.012
miR−3116	Inverse variance weighted	5	1.244 (1.046 to 1.479)	0.013
miR−22−5p	Inverse variance weighted	10	1.499 (1.086 to 2.071)	0.014
miR−4420	Inverse variance weighted	15	1.115 (1.022 to 1.217)	0.014
miR−1587	Inverse variance weighted	8	1.212 (1.036 to 1.419)	0.017
miR−616−3p	Inverse variance weighted	14	1.136 (1.023 to 1.261)	0.017
miR−224−3p	Inverse variance weighted	14	1.111 (1.017 to 1.215)	0.020
miR−548ba	Inverse variance weighted	10	1.130 (1.019 to 1.253)	0.021
miR−6823−5p	Inverse variance weighted	12	1.129 (1.018 to 1.252)	0.022
miR−301a−5p	Inverse variance weighted	16	1.107 (1.014 to 1.208)	0.023
miR−7108−5p	Inverse variance weighted	29	1.111 (1.014 to 1.217)	0.024
miR−4783−3p	Inverse variance weighted	10	1.117 (1.014 to 1.231)	0.025
miR−7112−3p	Inverse variance weighted	7	1.142 (1.016 to 1.283)	0.026
miR−212−5p	Inverse variance weighted	10	1.139 (1.014 to 1.280)	0.028
miR−4446−5p	Inverse variance weighted	13	1.136 (1.012 to 1.274)	0.030
miR−196b−5p	Inverse variance weighted	12	1.159 (1.014 to 1.325)	0.030
miR−6789−5p	Inverse variance weighted	5	1.508 (1.040 to 2.187)	0.030
miR−624−5p	Inverse variance weighted	25	1.081 (1.007 to 1.160)	0.031
miR−4256	Inverse variance weighted	20	1.090 (1.007 to 1.180)	0.032
miR−8058	Inverse variance weighted	8	1.134 (1.009 to 1.275)	0.035
miR−4496	Inverse variance weighted	12	1.122 (1.008 to 1.249)	0.035
miR−6769a−3p	Inverse variance weighted	11	1.158 (1.009 to 1.328)	0.036
miR−6501−3p	Inverse variance weighted	13	1.124 (1.007 to 1.255)	0.038
miR−6839−5p	Inverse variance weighted	11	1.123 (1.006 to 1.254)	0.038
miR−8071	Inverse variance weighted	4	1.247 (1.011 to 1.537)	0.039
miR−655−5p	Inverse variance weighted	8	1.144 (1.007 to 1.299)	0.039
miR−30e−3p	Inverse variance weighted	8	1.402 (1.016 to 1.935)	0.040
miR−4677−3p	Inverse variance weighted	15	1.089 (1.004 to 1.181)	0.040
miR−6758−3p	Inverse variance weighted	13	1.105 (1.003 to 1.217)	0.043
miR−629−5p	Inverse variance weighted	11	1.245 (1.007 to 1.540)	0.043
miR−3912−5p	Inverse variance weighted	6	1.439 (1.011 to 2.047)	0.043
miR−4452	Inverse variance weighted	14	1.103 (1.002 to 1.214)	0.045
miR−614	Inverse variance weighted	13	1.108 (1.002 to 1.226)	0.047

Figure 2. The causal association between all microRNAs and CRC for risk factor with CRC. We selected IVW as a primary method p<0.05 showed statistically significant; OR value >1 indicated a risk factor.

Exposure	Method	No.of SNP	OR(95% CI)	P
miR−484	Inverse variance weighted	15	0.558 (0.395 to 0.787)	0.001
miR−3192−3p	Inverse variance weighted	10	0.836 (0.748 to 0.935)	0.002
miR−6856−3p	Inverse variance weighted	11	0.862 (0.783 to 0.950)	0.003
miR−8069	Inverse variance weighted	105	0.948 (0.916 to 0.982)	0.003
miR−7976	Inverse variance weighted	5	0.790 (0.671 to 0.931)	0.005
miR−539−3p	Inverse variance weighted	7	0.844 (0.749 to 0.950)	0.005
miR−3198	Inverse variance weighted	13	0.875 (0.791 to 0.968)	0.009
miR−320e	Inverse variance weighted	6	0.646 (0.463 to 0.902)	0.010
miR−4439	Inverse variance weighted	8	0.855 (0.757 to 0.966)	0.012
miR−4655−5p	Inverse variance weighted	14	0.804 (0.672 to 0.962)	0.017
miR−5089−3p	Inverse variance weighted	5	0.829 (0.711 to 0.968)	0.017
miR−4719	Inverse variance weighted	11	0.904 (0.831 to 0.984)	0.019
miR−605−3p	Inverse variance weighted	14	0.891 (0.808 to 0.981)	0.019
miR−2467−5p	Inverse variance weighted	10	0.899 (0.822 to 0.984)	0.021
miR−520a−5p	Inverse variance weighted	10	0.892 (0.809 to 0.984)	0.023
miR−486−5p	Inverse variance weighted	7	0.681 (0.488 to 0.951)	0.024
miR−2115−5p	Inverse variance weighted	12	0.768 (0.610 to 0.967)	0.025
miR−34c−5p	Inverse variance weighted	18	0.877 (0.782 to 0.985)	0.026
miR−7162−5p	Inverse variance weighted	15	0.920 (0.854 to 0.991)	0.028
miR−6817−5p	Inverse variance weighted	10	0.889 (0.801 to 0.988)	0.029
miR−6741−5p	Inverse variance weighted	7	0.787 (0.634 to 0.976)	0.029
miR−6736−3p	Inverse variance weighted	7	0.804 (0.660 to 0.978)	0.029
miR−6796−3p	Inverse variance weighted	9	0.763 (0.598 to 0.973)	0.030
miR−300	Inverse variance weighted	15	0.913 (0.841 to 0.992)	0.031
miR−4320	Inverse variance weighted	16	0.911 (0.836 to 0.992)	0.033
miR−4668−5p	Inverse variance weighted	6	0.851 (0.733 to 0.987)	0.034
miR−5090	Inverse variance weighted	18	0.923 (0.857 to 0.994)	0.034
miR−1908−5p	Inverse variance weighted	4	0.770 (0.603 to 0.982)	0.035
miR−6773−5p	Inverse variance weighted	7	0.871 (0.765 to 0.992)	0.038
miR−16−5p	Inverse variance weighted	34	0.783 (0.621 to 0.989)	0.040
miR−6846−5p	Inverse variance weighted	12	0.882 (0.781 to 0.995)	0.041
miR−662	Inverse variance weighted	15	0.898 (0.809 to 0.996)	0.043
miR−4722−3p	Inverse variance weighted	11	0.865 (0.752 to 0.996)	0.043
miR−3134	Inverse variance weighted	8	0.881 (0.779 to 0.996)	0.043
miR−4457	Inverse variance weighted	9	0.891 (0.796 to 0.997)	0.044
miR−586	Inverse variance weighted	11	0.912 (0.834 to 0.998)	0.044
miR−574−5p	Inverse variance weighted	8	0.706 (0.502 to 0.992)	0.045
miR−8060	Inverse variance weighted	18	0.920 (0.847 to 0.999)	0.046
miR−2052	Inverse variance weighted	12	0.907 (0.823 to 0.999)	0.047
miR−370−3p	Inverse variance weighted	9	0.813 (0.662 to 0.999)	0.049
miR−6516−3p	Inverse variance weighted	14	0.917 (0.842 to 1.000)	0.049
miR−33a−5p	Inverse variance weighted	9	0.755 (0.571 to 1.000)	0.050
miR−7973	Inverse variance weighted	9	0.883 (0.780 to 1.000)	0.050

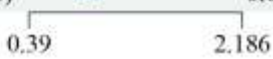

Figure 3. The causal association between all microRNAs and CRC for protective factor with CRC. We selected IVW as a primary method p<0.05 showed statistically significant; OR value <1 indicated a protective factor.

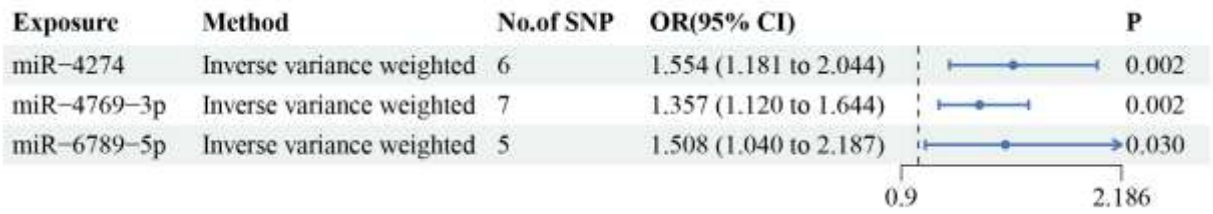

Figure 4. The causal association between three microRNAs and CRC. We selected IVW as a primary method p<0.05 showed statistically significant; OR value >1 indicated a risk factor, while OR value <1 indicated a protective factor.

Furthermore, a sensitivity analysis was performed. No heterogeneity was observed, with significant results from Cochran's Q test (P > 0.05), the causal estimates remained robust when analyzed using the random-effects inverse variance weighting (IVW) model (**Table 1**).

Table 1. The heterogeneity of causal association between all microRNAs and CRC. The p-values for the Cochran's Q yielded were above 0.05, suggesting that no significant heterogeneity effects were found.

exposure	method	Q	Q_df	Q_pval
miR-130a-3p	MR Egger	7,936359429	8	0,439711342
miR-130a-3p	Inverse variance weighted	9,989650317	9	0,35132373
miR-484	MR Egger	10,58343806	13	0,645669292
miR-484	Inverse variance weighted	10,7534449	14	0,705287131
miR-5196-3p	MR Egger	6,250651915	7	0,510805984
miR-5196-3p	Inverse variance weighted	6,40801878	8	0,601627283
miR-4274	MR Egger	2,965926943	4	0,563543543
miR-4274	Inverse variance weighted	4,358981248	5	0,498969949
miR-3192-3p	MR Egger	3,660556728	8	0,886378026
miR-3192-3p	Inverse variance weighted	6,728579579	9	0,665354384
miR-4769-3p	MR Egger	5,640723542	5	0,342761617
miR-4769-3p	Inverse variance weighted	5,658179787	6	0,462548351
miR-6856-3p	MR Egger	7,423486181	9	0,593117343
miR-6856-3p	Inverse variance weighted	9,025380425	10	0,529696587
miR-8069	MR Egger	95,01968476	103	0,699959409
miR-8069	Inverse variance weighted	95,4509572	104	0,713373654
miR-3652	MR Egger	1,846038667	7	0,967868156
miR-3652	Inverse variance weighted	2,67065123	8	0,953297968
miR-1185-5p	MR Egger	8,403261596	12	0,752876512
miR-1185-5p	Inverse variance weighted	12,10785949	13	0,518819837
miR-7976	MR Egger	0,994775956	3	0,80251602
miR-7976	Inverse variance weighted	1,361686763	4	0,850825945
miR-539-3p	MR Egger	2,11109067	5	0,833569841
miR-539-3p	Inverse variance weighted	2,729322166	6	0,841971756
miR-7158-3p	MR Egger	10,9331458	9	0,280319319
miR-7158-3p	Inverse variance weighted	11,12284139	10	0,348027997
miR-4764-5p	MR Egger	2,510654504	7	0,926292636
miR-4764-5p	Inverse variance weighted	2,648377739	8	0,954452531
miR-3679-5p	MR Egger	7,047133303	9	0,632212028
miR-3679-5p	Inverse variance weighted	7,816278636	10	0,646777083

miR-3662	MR Egger	2,28308921	7	0,942526855
miR-3662	Inverse variance weighted	2,290461038	8	0,970787277
miR-3198	MR Egger	10,04405303	11	0,526428956
miR-3198	Inverse variance weighted	10,05669564	12	0,61098667
miR-320e	MR Egger	5,74376547	4	0,219118664
miR-320e	Inverse variance weighted	5,755637742	5	0,330727203
miR-4439	MR Egger	4,473356163	6	0,612896035
miR-4439	Inverse variance weighted	6,285816382	7	0,506800501
miR-6792-5p	MR Egger	1,75397825	3	0,625000614
miR-6792-5p	Inverse variance weighted	1,754084002	4	0,78087135
miR-3116	MR Egger	2,496713515	3	0,475885318
miR-3116	Inverse variance weighted	2,519027541	4	0,641231889
miR-22-5p	MR Egger	10,53030678	8	0,229758217
miR-22-5p	Inverse variance weighted	10,97264017	9	0,27758898
miR-4420	MR Egger	6,392702437	13	0,930686308
miR-4420	Inverse variance weighted	6,392849665	14	0,95559789
miR-1587	MR Egger	5,949742446	6	0,428843489
miR-1587	Inverse variance weighted	5,966969439	7	0,543611435
miR-4655-5p	MR Egger	4,00417044	12	0,983361019
miR-4655-5p	Inverse variance weighted	4,208795613	13	0,988760755
miR-616-3p	MR Egger	7,866394661	12	0,79548209
miR-616-3p	Inverse variance weighted	7,877560019	13	0,85148446
miR-5089-3p	MR Egger	4,494685633	3	0,212764807
miR-5089-3p	Inverse variance weighted	4,946994432	4	0,292779566
miR-4719	MR Egger	6,215483337	9	0,718173104
miR-4719	Inverse variance weighted	6,569434554	10	0,765371136
miR-605-3p	MR Egger	12,2597641	12	0,425049686
miR-605-3p	Inverse variance weighted	12,40640154	13	0,494633358
miR-224-3p	MR Egger	12,27585236	12	0,423787678
miR-224-3p	Inverse variance weighted	12,58097058	13	0,480674042
miR-548ba	MR Egger	3,5493926	8	0,895322665
miR-548ba	Inverse variance weighted	3,951197294	9	0,914595111
miR-2467-5p	MR Egger	8,797248535	8	0,359687623
miR-2467-5p	Inverse variance weighted	8,965398164	9	0,440474373
miR-6823-5p	MR Egger	8,077267775	10	0,621289623
miR-6823-5p	Inverse variance weighted	9,473731538	11	0,578251004
miR-520a-5p	MR Egger	2,967591734	8	0,936374831
miR-520a-5p	Inverse variance weighted	3,101932648	9	0,960116052
miR-301a-5p	MR Egger	13,76517274	14	0,467348536
miR-301a-5p	Inverse variance weighted	13,82468842	15	0,53886464
miR-486-5p	MR Egger	5,945548334	5	0,311553419
miR-486-5p	Inverse variance weighted	7,175208658	6	0,304947642
miR-7108-5p	MR Egger	30,22644059	27	0,304075893
miR-7108-5p	Inverse variance weighted	31,0439917	28	0,315130519
miR-4783-3p	MR Egger	7,686092642	8	0,464718418
miR-4783-3p	Inverse variance weighted	7,916151916	9	0,542617738
miR-2115-5p	MR Egger	6,036115168	10	0,812219927
miR-2115-5p	Inverse variance weighted	8,451064156	11	0,672418614
miR-7112-3p	MR Egger	6,121020886	5	0,294620577
miR-7112-3p	Inverse variance weighted	8,478761716	6	0,205082939

miR-34c-5p	MR Egger	25,87169072	16	0,055860587
miR-34c-5p	Inverse variance weighted	26,13080927	17	0,072110071
miR-7162-5p	MR Egger	7,517577804	13	0,873549045
miR-7162-5p	Inverse variance weighted	7,876956791	14	0,895637222
miR-212-5p	MR Egger	8,448689698	8	0,390911263
miR-212-5p	Inverse variance weighted	8,944239231	9	0,442437276
miR-6817-5p	MR Egger	5,261845117	8	0,729258205
miR-6817-5p	Inverse variance weighted	6,064841203	9	0,733411571
miR-6741-5p	MR Egger	3,407390013	5	0,637444653
miR-6741-5p	Inverse variance weighted	4,862788139	6	0,561528374
miR-6736-3p	MR Egger	3,435706325	5	0,633137622
miR-6736-3p	Inverse variance weighted	3,491579061	6	0,745089726
miR-6796-3p	MR Egger	2,836280404	7	0,899723258
miR-6796-3p	Inverse variance weighted	2,840537493	8	0,943962462
miR-4446-5p	MR Egger	17,48730337	11	0,094264954
miR-4446-5p	Inverse variance weighted	19,60587561	12	0,074918514
miR-196b-5p	MR Egger	8,373151513	10	0,592437828
miR-196b-5p	Inverse variance weighted	9,24711165	11	0,599094401
miR-6789-5p	MR Egger	4,154167415	3	0,245290843
miR-6789-5p	Inverse variance weighted	4,323934598	4	0,363937583
miR-300	MR Egger	15,61913521	13	0,270309332
miR-300	Inverse variance weighted	15,62082067	14	0,337074334
miR-624-5p	MR Egger	28,50307218	23	0,197353831
miR-624-5p	Inverse variance weighted	28,68711087	24	0,232129022
miR-4256	MR Egger	14,39642816	18	0,702907065
miR-4256	Inverse variance weighted	14,90465895	19	0,728637435
miR-4320	MR Egger	12,2548116	14	0,585847589
miR-4320	Inverse variance weighted	13,83355134	15	0,538188668
miR-4668-5p	MR Egger	3,206487786	4	0,523883696
miR-4668-5p	Inverse variance weighted	4,418316377	5	0,490886241
miR-5090	MR Egger	14,4812793	16	0,562906404
miR-5090	Inverse variance weighted	15,06936345	17	0,590485378
miR-8058	MR Egger	5,936993582	6	0,430285043
miR-8058	Inverse variance weighted	6,268994245	7	0,508714884
miR-4496	MR Egger	3,991200586	10	0,947743066
miR-4496	Inverse variance weighted	5,285276073	11	0,916567468
miR-1908-5p	MR Egger	0,131703809	2	0,936269511
miR-1908-5p	Inverse variance weighted	0,169690786	3	0,982327218
miR-6769a-3p	MR Egger	4,33169072	9	0,888257662
miR-6769a-3p	Inverse variance weighted	4,652309605	10	0,913162247
miR-6773-5p	MR Egger	5,216247261	5	0,390063296
miR-6773-5p	Inverse variance weighted	5,236011656	6	0,513918758
miR-6501-3p	MR Egger	16,10807898	11	0,13716568
miR-6501-3p	Inverse variance weighted	16,41672877	12	0,17288581
miR-6839-5p	MR Egger	7,176719363	9	0,61872618
miR-6839-5p	Inverse variance weighted	7,297605551	10	0,697082061
miR-8071	MR Egger	1,028958563	2	0,597811805
miR-8071	Inverse variance weighted	1,148514173	3	0,765377326
miR-655-5p	MR Egger	2,019040437	6	0,917939147
miR-655-5p	Inverse variance weighted	2,356593072	7	0,937503259

miR-30e-3p	MR Egger	3,52368182	6	0,740816313
miR-30e-3p	Inverse variance weighted	4,233708962	7	0,75249957
miR-16-5p	MR Egger	38,57827579	32	0,196558342
miR-16-5p	Inverse variance weighted	39,12821482	33	0,213858266
miR-4677-3p	MR Egger	7,330804233	13	0,884308797
miR-4677-3p	Inverse variance weighted	7,761377185	14	0,901383474
miR-6846-5p	MR Egger	12,01206924	10	0,284249563
miR-6846-5p	Inverse variance weighted	12,23586145	11	0,346178007
miR-6758-3p	MR Egger	8,88754811	11	0,632271438
miR-6758-3p	Inverse variance weighted	8,896191445	12	0,711770577
miR-662	MR Egger	5,190016349	13	0,970768397
miR-662	Inverse variance weighted	8,878957428	14	0,838725494
miR-629-5p	MR Egger	10,91309761	9	0,281712745
miR-629-5p	Inverse variance weighted	10,98898953	10	0,358376465
miR-3912-5p	MR Egger	2,87447793	4	0,579046127
miR-3912-5p	Inverse variance weighted	7,111439753	5	0,212483455
miR-4722-3p	MR Egger	5,487301545	9	0,789930419
miR-4722-3p	Inverse variance weighted	5,519578749	10	0,853883897
miR-3134	MR Egger	5,857216111	6	0,439373586
miR-3134	Inverse variance weighted	6,178410205	7	0,519078817
miR-4457	MR Egger	4,800085158	7	0,684344567
miR-4457	Inverse variance weighted	6,207468843	8	0,624004693
miR-586	MR Egger	4,293280489	9	0,891071297
miR-586	Inverse variance weighted	4,812428999	10	0,903350445
miR-4452	MR Egger	6,731087062	12	0,874860835
miR-4452	Inverse variance weighted	7,362258361	13	0,882530778
miR-574-5p	MR Egger	2,468411372	6	0,87198605
miR-574-5p	Inverse variance weighted	2,847119742	7	0,898775496
miR-8060	MR Egger	18,26640284	16	0,308529421
miR-8060	Inverse variance weighted	18,46587697	17	0,360036589
miR-614	MR Egger	14,36391672	11	0,213506413
miR-614	Inverse variance weighted	14,53947585	12	0,26759173
miR-2052	MR Egger	11,73194708	10	0,303396823
miR-2052	Inverse variance weighted	11,9273971	11	0,369125247
miR-370-3p	MR Egger	3,373384112	7	0,848448908
miR-370-3p	Inverse variance weighted	3,56194806	8	0,894329042
miR-6516-3p	MR Egger	6,560285533	12	0,885253122
miR-6516-3p	Inverse variance weighted	8,389198062	13	0,81735326
miR-33a-5p	MR Egger	5,315657863	7	0,621501803
miR-33a-5p	Inverse variance weighted	5,32714269	8	0,722106551
miR-7973	MR Egger	13,77901285	7	0,055254349
miR-7973	Inverse variance weighted	13,91180357	8	0,084093385

The P-values for the MR-Egger intercept were above 0.05, indicating no significant pleiotropic effects (**Table 2**).

Table 2. The pleiotropy of causal association between all microRNAs and CRC. The MR-Egger intercept p-values were >0.05, suggesting that no significant pleiotropy effects were found.

exposure	egger_intercept	se	pval

miR-130a-3p	0,019947441	0,013920728	0,189775
miR-5196-3p	0,011573924	0,029175881	0,70340827
miR-4274	0,033234282	0,02815803	0,303284088
miR-4769-3p	-0,00455718	0,036635586	0,90585099
miR-3652	-0,020833861	0,022942714	0,394022628
miR-1185-5p	-0,038927081	0,020224664	0,078294614
miR-7158-3p	0,009282513	0,023490284	0,701924304
miR-4764-5p	0,011633216	0,031347014	0,721531903
miR-3679-5p	-0,016323649	0,018612857	0,403283915
miR-3662	-0,002663704	0,031024038	0,933982453
miR-6792-5p	-0,001674218	0,162804352	0,992440636
miR-3116	-0,009377559	0,062777043	0,890731757
miR-22-5p	-0,012332174	0,021273566	0,578076188
miR-4420	-0,000235099	0,019375622	0,990503122
miR-1587	0,004659192	0,03549816	0,899866633
miR-616-3p	0,00165613	0,015673216	0,917592943
miR-224-3p	0,010864382	0,019893269	0,594982173
miR-548ba	-0,029597387	0,046692364	0,543852805
miR-6823-5p	-0,026919017	0,022779509	0,26465573
miR-301a-5p	0,00437838	0,017947242	0,810801865
miR-7108-5p	0,020794111	0,024332937	0,400310469
miR-4783-3p	-0,012036232	0,025094046	0,644318315
miR-7112-3p	0,064514414	0,046487442	0,223868574
miR-212-5p	0,016378368	0,023909846	0,512695226
miR-4446-5p	-0,024242513	0,021000087	0,272799448
miR-196b-5p	0,016540027	0,017692549	0,371886153
miR-6789-5p	-0,029035697	0,082925242	0,749372275
miR-624-5p	0,005813079	0,015084592	0,703507773
miR-4256	-0,009769508	0,013703838	0,485045973
miR-8058	-0,017645191	0,030623645	0,585432459
miR-4496	-0,040000772	0,035163215	0,281820357
miR-6769a-3p	0,012309937	0,021740087	0,585076343
miR-6501-3p	0,010501472	0,022874032	0,655101386
miR-6839-5p	0,007429232	0,021367591	0,736068331
miR-8071	0,024935073	0,072115009	0,762500569
miR-655-5p	-0,018178055	0,031287918	0,582395493
miR-30e-3p	-0,021990686	0,026097644	0,43173539
miR-4677-3p	0,014104212	0,021494406	0,523153108
miR-6758-3p	0,001741205	0,018728766	0,927599437
miR-629-5p	0,007726523	0,030884395	0,808068713
miR-3912-5p	-0,055482786	0,026954482	0,108651004
miR-4452	-0,016076048	0,020235115	0,44235505
miR-614	-0,01119254	0,030525095	0,720822985

Additionally, we further evaluated the data using scatter plots (**Fig. 5D-F**), funnel plots (**Fig. 6A-C**), and leave-one-out plots (**Fig. 6D-F**), which helped to eliminate the potential influence of outliers and horizontal pleiotropy on the identified key miRNAs. To further assess the influence of potential directional pleiotropy, we scanned each of the SNPs used as IVs for their potential secondary phenotypes using the GWAS Catalog (https://www.ebi.ac.uk/gwas/, last accessed on September 22, 2025), The results show no any SPN associated with CRC risk factors such as

smoking, alcohol consumption, body mass index, and inflammatory bowel disease in this study (**Table S2**).

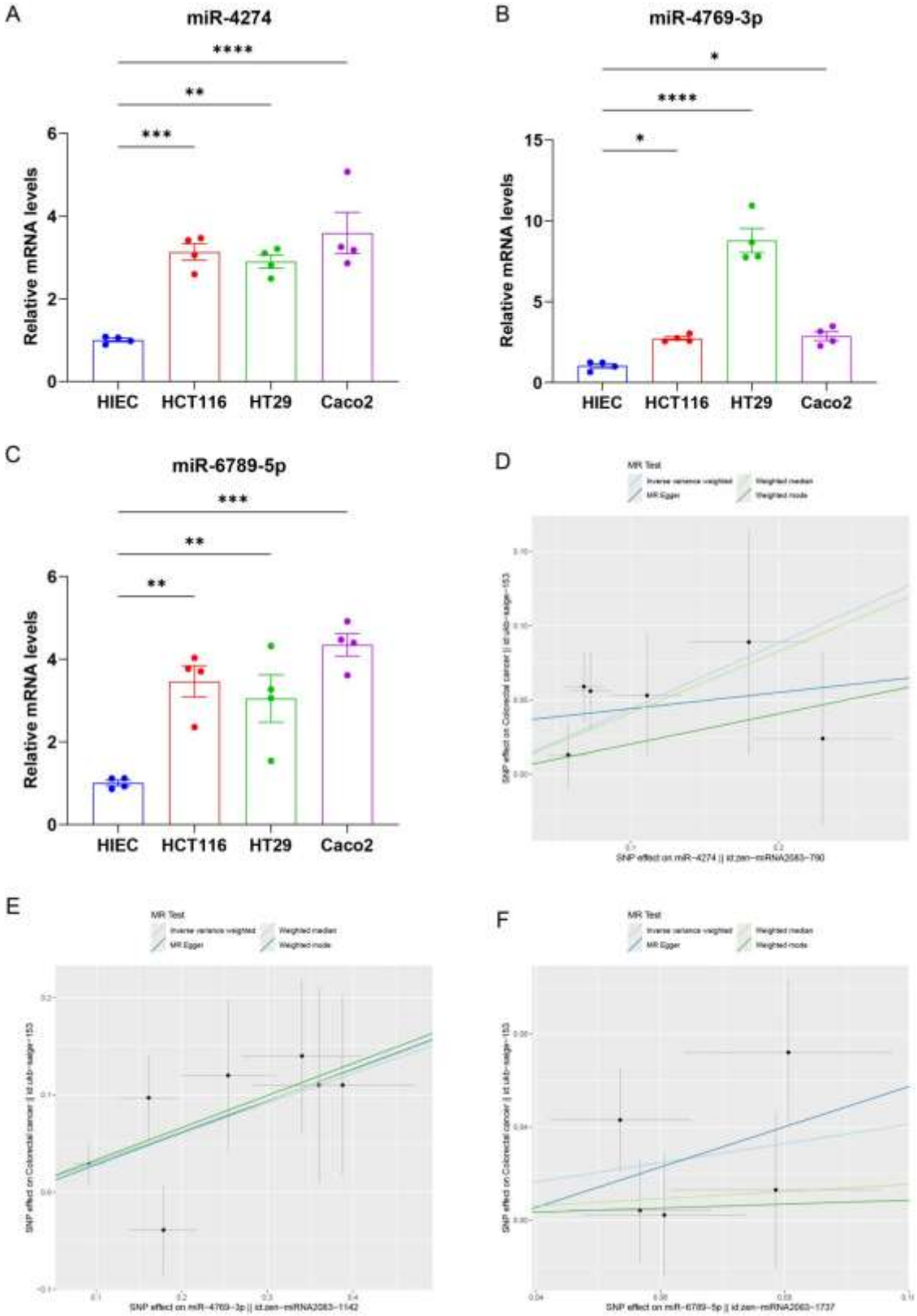

Figure 5. RT-qPCR in CRC; (A) miR-4274 expression is higher in CRC cell lines than in normal cells. (B) miR-4769-3p expression is higher in CRC cell lines than in normal cells. (C) miR-6789-5p expression is higher in CRC cell lines than in normal cells. (D) Scatter plot showing the relationship of miR-4274 with the risk of CRC. (E) Scatter plot showing the relationship of miR-4769-3p with the risk of CRC. (F) Scatter plot showing the relationship of miR-6789-5p with the risk of CRC.

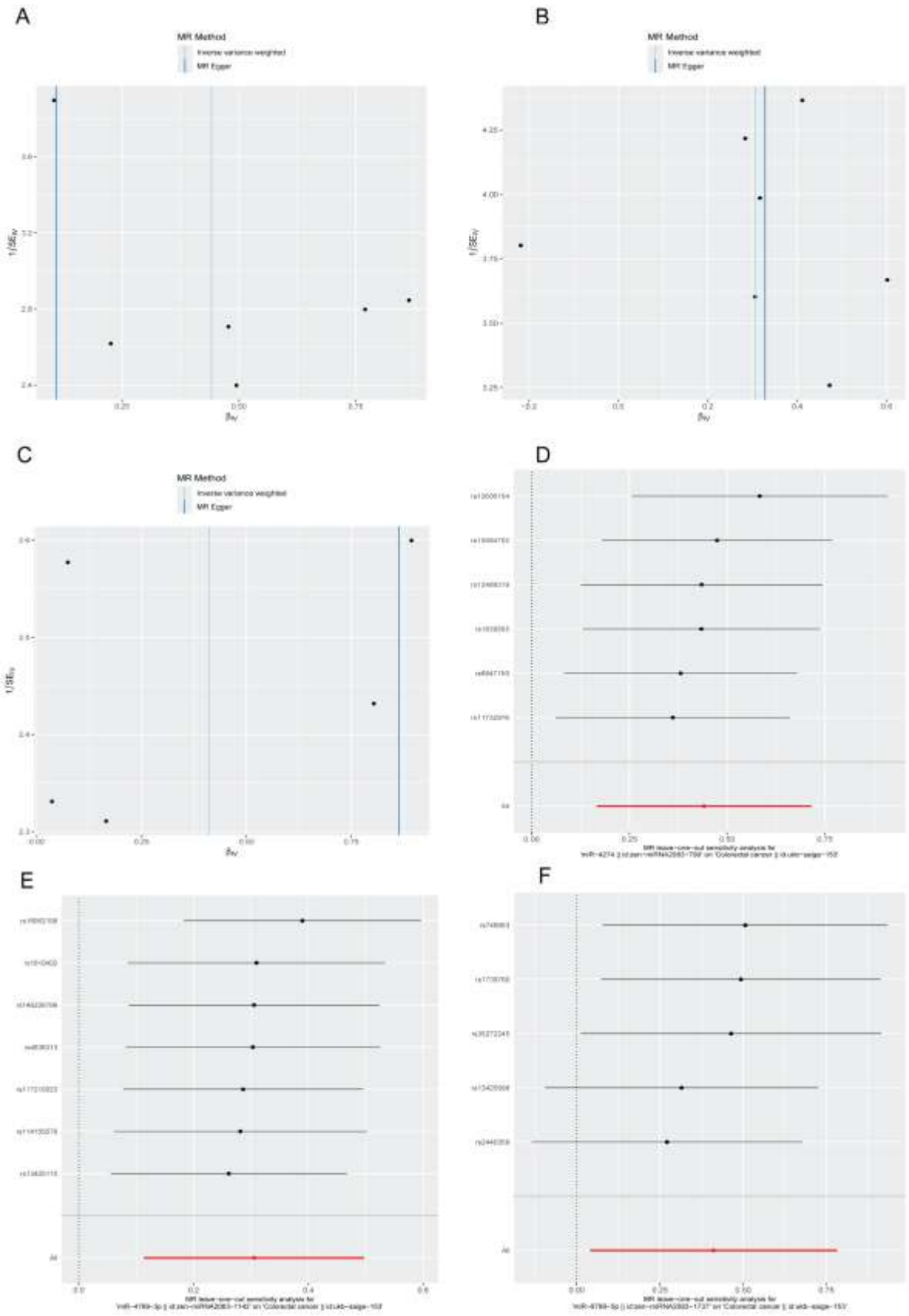

Figure 6. Funnel plot showing IVs for each significant causal association between three miRNAs and CRC. (A) miR-4274 in CRC. (B) miR-4769-3p in CRC. (C) miR-6789-5p in CRC. (D) Leave-one-out plot showing the genetic associations of miR-4274 in CRC;
(E) Leave-one-out plot showing the genetic associations of miR-4769-3p in CRC; (E) Leave-one-out plot showing the genetic associations of miR-6789-5p in CRC.

3.2 miR−4274, miR−4769−3p, and miR−6789−5p Real Time Quantitative PCR in CRC

In this experiment, we compared the expression differences of miR-4274, miR-4769-3p, and miR-6789-5p in CRC cells HCT116, HT29, and CACO2 and normal colon epithelial cells HIEC. The RT qPCR results showed that the expression levels of miR-4274, miR-4769-3p, and miR-6789-5p in HCT116, HT29, and CACO2 cells were significantly higher than those in HIEC cells. This result suggests that changes in miRNA expression levels may play an important role in the occurrence and development of CRC, potentially affecting the biological behavior of tumor cells and their differences from normal colon epithelial cells (**Fig. 5A-C; Table 3**).

Table 3. Summary of RT-qPCR results for miRNAs, presented as mean differences. Statistical significance compared with HIEC control cells is indicated by stars (ns = not significant; *P < 0.05, **P < 0.01, ***P < 0.001, ****P < 0.0001). Exact adjusted P-values and fold changes are provided.

Group	Comparison	Mean Diff	Summary	Adjusted P Value	Fold Change
miR4274	HIEC vs. HCT116	-2.13	***	0.0005	3.13
	HIEC vs. HT29	-1.897	**	0.0013	2.897
	HIEC vs. Caco2	-2.587	****	<0.0001	3.587
miR4769-3p	HIEC vs. HCT116	-1.696	*	0.0316	2.696
	HIEC vs. HT29	-7.755	****	<0.0001	8.755
	HIEC vs. Caco2	-1.838	*	0.0202	2.838
miR6789-5p	HIEC vs. HCT116	-2.457	**	0.0014	3.457
	HIEC vs. HT29	-2.039	**	0.0056	3.039
	HIEC vs. Caco2	-3.34	***	0.0001	4.34

4 Discussion

This study identified 86 miRNAs associated with CRC through Mendelian randomization (MR) analysis, including 43 risk-associated and 43 protective miRNAs. These findings highlight the dual regulatory roles of miRNAs in colorectal tumorigenesis. Dysregulated miRNAs in CRC participate in oncogenic and tumor-suppressive pathways, such as Wnt/β-catenin, PI3K/AKT, TGF-β, and p53, modulating proliferation, apoptosis, invasion, and immune evasion [22–26]. Beyond their mechanistic roles, miRNAs also hold promise as biomarkers for diagnosis, prognosis, and therapeutic targeting [27–29].

To illustrate these findings, we focused on three representative candidates—miR-4274, miR-4769-3p, and miR-6789-5p—that exhibited significant dysregulation in CRC cells.

4.1 Mechanistic Insights

Our analysis revealed that miR-4274 is highly expressed in CRC cells. Polymorphism in its seed region has been shown to influence the expression of the target gene PEX5 and enhance radiotherapy resistance [27], linking miR-4274 to DNA damage response and therapeutic resistance. Moreover, miR-4274 and its host gene SORCS2 regulate IGFBP6 in basal-like breast cancer, affecting tumor proliferation and migration [28], suggesting conserved roles across tumor types.

MiR-4769-3p has been reported to regulate apoptosis and energy metabolism through the USP18/VDAC2 pathway [29]. While studied in systemic sclerosis, this mechanism implies potential involvement in CRC metabolic reprogramming and cell survival. Similarly, miR-6789-5p is suppressed by LINC00273 in triple-negative breast cancer, promoting metastasis and stemness [30]. Together, these findings suggest that miR-4769-3p and miR-6789-5p may contribute to CRC progression through metabolic and stemness-related mechanisms.

4.2 Clinical Relevance

The mechanistic roles of these miRNAs suggest potential clinical implications. MiR-4274 polymorphisms have been associated with gastric cancer susceptibility [31] and radiotherapy resistance in CRC [27], highlighting its value as a predictive biomarker for risk and treatment outcomes. Circulating miR-4769-3p is elevated in the serum of non-small cell lung cancer patients

[32], indicating potential as a non-invasive biomarker applicable to CRC. The involvement of miR-6789-5p in tumor metastasis and stemness [30] further underscores its potential as a therapeutic target in advanced CRC.

4.3 Limitations and Future Directions

Despite these promising findings, the precise downstream targets and signaling pathways of miR-4274, miR-4769-3p, and miR-6789-5p in CRC remain to be experimentally validated. Functional studies employing knockdown or overexpression systems combined with transcriptomic and proteomic profiling are warranted. Additionally, large-scale clinical validation is needed to assess their diagnostic and prognostic utility. Integration of liquid biopsy technologies may facilitate translation into precision medicine by enabling dynamic disease monitoring and treatment stratification [33,34].

5 Strengths and Limitations

This study has several notable strengths. MR provides a robust framework to emulate randomized controlled trials using observational data, effectively mitigating reverse causation and confounding. Extensive sensitivity analyses revealed no substantial heterogeneity or horizontal pleiotropy, supporting the robustness of our findings.

Our study systematically applied MR to investigate the potential causal effects of circulating miRNAs on CRC, identifying three miRNAs with potential causal effects and 86 additional miRNAs showing nominal associations with CRC-related outcomes. These results highlight the potential of miRNAs as novel biomarkers for CRC prevention and treatment.

The study has limitations. First, miRNA eQTL data were derived from a European-only population, potentially introducing population bias. Second, RT-qPCR validation was performed only in CRC cell lines (HIEC, HCT116, HT29, and Caco2); studies using primary tissues or additional models are needed to enhance biological generalizability.

6 Conclusions

In summary, this study emphasizes the key role of miRNAs in CRC. MR screening confirmed that the expression of these miRNAs is closely related to CRC occurrence, progression, and prognosis, providing insights into underlying molecular mechanisms. These miRNAs, as potential biomarkers, could be used for early diagnosis, prognostic evaluation, and as targets for future therapeutic interventions.

Availability of Data and Materials

All the data for the present article can be found on the GWAS (http://www.ebi.ac.uk/gwas/) and the UK Biobank (www.ukbiobank.ac.uk).

Author Contribution

Z. P. and **A. P.** were responsible for data acquisition, analysis, interpretation, and drafting of the manuscript. **M. W.** and **P. N.** contributed to study design, manuscript revision, and overall guidance. All authors approved the final manuscript.

Funding

None.

Declarations

- **Ethical Approval:** Not applicable. This study used publicly available, de-identified summary-level data from the GWAS Catalog and UK Biobank.
- **Consent to Participate**: Not applicable.
- **Consent to Publish:** Not applicable.
- **Clinical Trial Number:** Not applicable.
- **Competing Interests:** The authors declare that they have no competing interests.

Abbreviations

CI: Confidence Interval

CRC: Colorectal Cancer

Ct: Cycle threshold

ΔΔCt: Delta Delta Ct

FDR: False Discovery Rate

FHS: Framingham Heart Study

GWAS: Genome-Wide Association Study

IV: Instrumental Variable

IVW: Inverse Variance Weighted

LD: Linkage Disequilibrium

miRNA: microRNA

miR-eQTL: MicroRNA Expression Quantitative Trait Locus

MR: Mendelian Randomization

NSCLC: Non-Small Cell Lung Cancer

OR: Odds Ratio

P-RT: Poly(A) Tail Reverse Transcription

Qpcr: Quantitative Polymerase Chain Reaction

SNP: Single-Nucleotide Polymorphism

UKB: UK Biobank

References

1. Sung, H., et al., Global Cancer Statistics 2020: GLOBOCAN Estimates of Incidence and Mortality Worldwide for 36 Cancers in 185 Countries. CA Cancer J Clin, 2021. **71**(3): p. 209-249.
2. Pierantoni, C., L. Cosentino, and L. Ricciardiello, Molecular Pathways of Colorectal Cancer Development: Mechanisms of Action and Evolution of Main Systemic Therapy Compunds. Dig Dis, 2024. **42**(4): p. 319-324.
3. Peng, Y. and C.M. Croce, *The role of MicroRNAs in human cancer.* Signal Transduct Target Ther, 2016. **1**: p. 15004.
4. Liang, C., et al., Recent advances in the diagnostic and therapeutic roles of microRNAs in colorectal cancer progression and metastasis. Front Oncol, 2022. **12**: p. 911856.
5. Zhang, Y., et al., CircRNAs in colorectal cancer: potential biomarkers and therapeutic targets. Cell Death Dis, 2023. **14**(6): p. 353.
6. Xu, P., et al., Colorectal cancer characterization and therapeutic target prediction based on microRNA expression profile. Sci Rep, 2016. **6**: p. 20616.
7. Li, J., et al., Serum miRNA expression profile as a prognostic biomarker of stage II/III colorectal adenocarcinoma. Sci Rep, 2015. **5**: p. 12921.
8. Dong, J., J.W. Tai, and L.F. Lu, *miRNA-Microbiota Interaction in Gut Homeostasis and Colorectal Cancer.* Trends Cancer, 2019. **5**(11): p. 666-669.
9. Davey Smith, G. and G. Hemani, Mendelian randomization: genetic anchors for causal inference in epidemiological studies. Hum Mol Genet, 2014. **23**(R1): p. R89-98.
10. Huan, T., et al., Genome-wide identification of microRNA expression quantitative trait loci. Nat Commun, 2015. **6**: p. 6601.
11. Sidore, C., et al., Genome sequencing elucidates Sardinian genetic architecture and augments association analyses for lipid and blood inflammatory markers. Nat Genet, 2015. **47**(11): p. 1272-1281.
12. Sun, Y., J. Zhou, and K. Ye, White Blood Cells and Severe COVID-19: A Mendelian Randomization Study. J Pers Med, 2021. **11**(3).
13. Davies, N.M., M.V. Holmes, and G. Davey Smith, Reading Mendelian randomisation studies: a guide, glossary, and checklist for clinicians. Bmj, 2018. **362**: p. k601.
14. Hartwig, F.P., G. Davey Smith, and J. Bowden, Robust inference in summary data Mendelian randomization via the zero modal pleiotropy assumption. Int J Epidemiol, 2017. **46**(6): p. 1985-1998.
15. Bowden, J., et al., Consistent Estimation in Mendelian Randomization with Some Invalid Instruments Using a Weighted Median Estimator. Genet Epidemiol, 2016. **40**(4): p. 304-14.
16. Allen, R.J., et al., Genetic variants associated with susceptibility to idiopathic pulmonary fibrosis in people of European ancestry: a genome-wide association study. Lancet Respir

Med, 2017. **5**(11): p. 869-880.
17. Baicus, C., White Blood Cells, COVID-19, and Mendelian Randomization. J Pers Med, 2022. **12**(9).
18. Verbanck, M., et al., Detection of widespread horizontal pleiotropy in causal relationships inferred from Mendelian randomization between complex traits and diseases. Nat Genet, 2018. **50**(5): p. 693-698.
19. Hemani, G., K. Tilling, and G. Davey Smith, Orienting the causal relationship between imprecisely measured traits using GWAS summary data. PLoS Genet, 2017. **13**(11): p. e1007081.
20. Hemani, G., et al., The MR-Base platform supports systematic causal inference across the human phenome. Elife, 2018. **7**.
21. Yavorska, O.O. and S. Burgess, MendelianRandomization: an R package for performing Mendelian randomization analyses using summarized data. Int J Epidemiol, 2017. **46**(6): p. 1734-1739.
22. Calin, G.A. and C.M. Croce, *MicroRNA-cancer connection: the beginning of a new tale.* Cancer Res, 2006. **66**(15): p. 7390-4.
23. Bartel, D.P., MicroRNAs: target recognition and regulatory functions. Cell, 2009. **136**(2): p. 215-33.
24. Monroig-Bosque Pdel, C., C.A. Rivera, and G.A. Calin, *MicroRNAs in cancer therapeutics: "from the bench to the bedside".* Expert Opin Biol Ther, 2015. **15**(10): p. 1381-5.
25. To, K.K., et al., MicroRNAs in the prognosis and therapy of colorectal cancer: From bench to bedside. World J Gastroenterol, 2018. **24**(27): p. 2949-2973.
26. Lorusso, C., et al., miRNAs as Key Players in the Management of Cutaneous Melanoma. Cells, 2020. **9**(2).
27. Lu, Q., et al., Polymorphism in the Hsa-miR-4274 seed region influences the expression of PEX5 and enhances radiotherapy resistance in colorectal cancer. Front Med, 2024. **18**(5): p. 921-937.
28. Shkurnikov, M., et al., LAMA4-Regulating miR-4274 and Its Host Gene SORCS2 Play a Role in IGFBP6-Dependent Effects on Phenotype of Basal-Like Breast Cancer. Front Mol Biosci, 2019. **6**: p. 122.
29. Tang, B., et al., MiR-4769-3p suppresses adipogenesis in systemic sclerosis by negatively regulating the USP18/VDAC2 pathway. iScience, 2024. **27**(8): p. 110483.
30. Sengupta, P., et al., Long non-coding intergenic RNA, LINC00273 induces cancer metastasis and stemness via miRNA sponging in triple negative breast cancer. Int J Biol Macromol, 2024. **274**(Pt 1): p. 132730.
31. Landeros, N., et al., Novel Risk Associations between microRNA Polymorphisms and Gastric Cancer in a Chilean Population. Int J Mol Sci, 2021. **23**(1).
32. Zhang, X., et al., Identification of serum MiRNAs as candidate biomarkers for non-small cell lung cancer diagnosis. BMC Pulm Med, 2022. **22**(1): p. 479.
33. Casagrande, G.M.S., et al., Liquid Biopsy for Lung Cancer: Up-to-Date and Perspectives for Screening Programs. Int J Mol Sci, 2023. **24** (3).
34. Bao, Y., et al., Beyond blood: Advancing the frontiers of liquid biopsy in oncology and personalized medicine. Cancer Sci, 2024. **115** (4): p. 1060-1072.